A Mathematical Model On The Dynamics Of Radioactive Tracer Flow In PET Scan*

Saqib Mubarak†, Mukhtar Ahmad Khanday‡

Abstract

The use of tracers in certain imaging techniques are vital for the diagnosis, prevention and treatment of various diseases. The role of mathematical modeling in positron emission tomography (PET) scans provides an optimal information about the functioning of organs in terms of flow and concentration profiles of the radioactive tracer material infused through bloodstream. In this paper, some new, innovative and efficient solutions of a frequently used model in tracer kinetics are presented. Two solutions are discussed with unknown and known input data of radioactive tracers. It has been observed that the first solution with unknown input data can be obtained from the second solution with known data. The transport and diffusion of tracer material through various compartments have been analysed and modelled using law of conservation of energy, fundamental matrices, eigenvalues and eigenfunctions. The results obtained can help technicians of nuclear medicine to evaluate the PET data while scanning and diagnosis to understand various other parameters like the standardized uptake value (SUV), fractional uptake rate (FUR), and the distribution volume (DV). The concentration and flow of radioactive tracer are computed at various regions using first order kinetics and thereby easily determine the other essential parameters required in PET. The method is analytical and the results are simulated graphically using the Wolfram MATHEMATICA software and are compared to the already published/experimental data to depict the efficacy of the solutions.

1 Introduction

For diagnostic purposes of various diseases, radiotracers are injected intravenously in the bloodstream of human body (see [10], [11]). Their time-activity and distribution profiles are used to track the progress or history of some diseases or other biological processes, using certain imaging techniques done through positron emission tomography (PET). To this perspective, mathematical models provide detailed insights and help determining such profiles (see Peppas and Narsimhan [1]). For determining the time-activity profiles of the radiotracers, various mathematical models have already been developed, followed by experimental verifications.

The PET data applied to reversible and irreversible tracers was graphically analyzed by Logan [4]. In his work, the input function is assumed as an uptake data from a region of interest (ROI). Further the model used in his work is a three-compartment reversible model. The same model was studied by Bentourkia and Zaidi [6], where the model solutions are presented analytically using the convolution integrals, to determine the corresponding radioactive concentrations in each compartment of the used-model. The time-activity profiles of a particular radiotracer in tumor imaging, using the mathematical modeling, have also been determined by Shevtsova's [8].

The most frequently used compartmental model in tracer kinetics is as shown in Figure 1 and can be seen in the literature (see Watabe et al. [5], Nguyen et al. [7], and Phair [9]). To determine the corresponding profiles and parameters through PET, using this model, the main fun lies in determining the structure of

the input function (injected tracer), and hence the other tracer-concentrations in the corresponding compartments. Till date, either the input function is chosen explicitly as a function of time, some numerical value is considered or the methods used to determine the same are capricious and hectic (see Lau et al. [2]). Furthermore, the time-activity profiles obtained, using the above mentioned values of the input function, are evaluated either implicitly or explicitly in terms of the convolution integrals. Hence, such profiles and solutions are hectic and more time-consuming to evaluate, leading to less accurate and capricious solutions.

However, in this work, two new solutions of the same model, shown in Figure 1 are presented. The first solution is obtained with an unknown input and is hence itself a method in determining the same. The second solution is obtained using a known input. Both solutions are obtained using the fundamental matrix method. These solutions are easy to evaluate, analytic and most accurate as compared to other methods. The results are simulated graphically using the Wolfram MATHEMATICA software and are compared to the already published/experimental data (see Tantawy et al. [3], Logan [4] and Phair [9]) to depict the efficacy of the solutions. Hence, this work has tangible applications in nuclear medicine and other imaging/scanning studies done through PET. Also, it can help to determine the concentration/time-activity profiles and other essential parameters required, while diagnosing and obtaining PET data.

2   Materials and Methods

During a typical PET study, PET data is subsequently obtained after the radiotracer is administered intravenously with respect to time. For diagnosing a particular disease or its progress done through PET, various parameters are needed (see Watabe et al. [5]). To this purpose, the differential equations of the compartmental analysis are the basis of the models describing the uptake of tracers used in imaging studies. The compartmental model used to understand the dynamics of tracer material in biological tissues is shown in Figure 1, where the first compartment represents the tracer input $C_p(t)$, administered intravenously. From
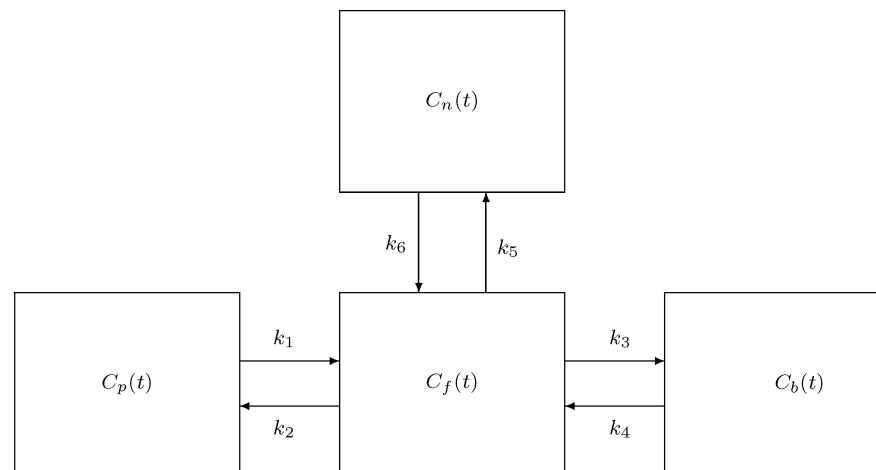

Figure 1: General three-tissue(or four compartments) compartmental model (see Watabe et al. [5]). The model consists of the compartments plasma $C_p(t)$ (input), free radiotracer in tissue $C_f(t)$, specific binding tracer in tissue $C_b(t)$ and non-specific binding tracer in tissue $C_n(t)$, and the tracer-transfer constants $k_1 - k_6$.

this compartment, the radio-tracer moves into the free compartment $C_f(t)$. Thereafter, this compartment interacts with two more compartments $C_b(t)$, which represents the region of specific binding of the radio-tracer and $C_n(t)$, which is the non-specific binding compartment. The transfer of the tracer concentrations between the corresponding compartments is linearly given in terms of the rate constants $k_1 - k_6$ (see Watabe et al. [5], Bentourkia and Zaidi [6] and Nguyen et al. [7]) and is determined by the application of law of conservation of mass and the first order kinetics. The proportionality and the transfer coefficients depend

upon the radiotracer injected, the compartment, the individual under diagnosis and the region of interest (ROI), which is to be diagnosed. If the tracer-concentration in any compartment j is $C_j(t)$ at any time t, then by the law of conservation of mass, the rate of change of $C_j(t)$ is

$$\frac{dC_j}{dt} = \text{Inlet tracer amount} - \text{Outlet tracer amount}. \tag{1}$$

2.1 Solution with Unknown Input

If the input $C_p(t)$ is unknown, Eqn. (1), applied to each of the compartments, yields a homogeneous system of four linear differential equations as

$$\frac{dC_p(t)}{dt} = -k_1 C_p(t) + k_2 C_f(t); \ C_p(0) = C_0, \tag{2}$$

$$\frac{dC_f(t)}{dt} = k_1 C_p(t) - (k_2 + k_3 + k_5)C_f(t) + k_4 C_b(t) + k_6 C_n(t); \ C_f(0) = 0, \tag{3}$$

$$\frac{dC_b(t)}{dt} = k_3 C_f(t) - k_4 C_b(t); \ C_b(0) = 0, \tag{4}$$

$$\frac{dC_n(t)}{dt} = k_5 C_f(t) - k_6 C_n(t); \ C_n(0) = 0, \tag{5}$$

where C_0 is the initial concentration of the injected tracer. The above system is written in the matrix form as

$$\frac{dC(t)}{dt} = MC(t); \ C(0) = X_0 \tag{6}$$

where

$$C(t) = \begin{bmatrix} C_p(t) \\ C_f(t) \\ C_b(t) \\ C_n(t) \end{bmatrix}, \ M = \begin{bmatrix} -k_1 & k_2 & 0 & 0 \\ k_1 & -(k_2+k_3+k_5) & k_4 & k_6 \\ 0 & k_3 & -k_4 & 0 \\ 0 & k_5 & 0 & -k_6 \end{bmatrix}, \ X_0 = \begin{bmatrix} C_0 \\ 0 \\ 0 \\ 0 \end{bmatrix}.$$

Now, if $F(t)$ is the fundamental matrix (see Ross [12] and Hartman [13]) corresponding to the homogeneous system given in Eqn. (6), the solution of this initial value problem is given as

$$C(t) = F(t)F(0)^{-1}X_0. \tag{7}$$

Eqn. (7) determines explicitly the input function $C_p(t)$ and all the other radiotracer concentrations in every compartment. These concentration-profiles are in turn used to obtain the time-activity profiles and other essential parameters required during PET scanning. So, this solution has the benefit in itself that it can be used to such a compartmental model without knowing the input and most importantly, the solution also gives a method to determine the structure of the input function. The forthcoming case-study elaborates the determination of these functions and other parameters explicitly, obtained using this solution method.

Case-Study:

In order to determine the time-activity profiles of all the radiotracer concentrations and the input function, we consider the particular values of the parameters and transfer-coefficients mentioned in the work of Logan [4]: $k_1 = 0.5$ min^{-1}, $k_2 = 0.125$ min^{-1}, $k_3 = 0.2$ min^{-1}, $k_4 = 0.005$ min^{-1}, $k_5 = 0.0.28$ min^{-1}, $k_6 = 0.17$ min^{-1}, $C_0 = 1$ mg. Using these values, M takes the form

$$M = \begin{bmatrix} -0.5 & 0.125 & 0 & 0 \\ 0.5 & -0.605 & 0.005 & 0.17 \\ 0 & 0.2 & -0.005 & 0 \\ 0 & 0.28 & 0 & -0.17 \end{bmatrix}.$$

Now the eigenvalues of M are evaluated, using the Wolfram MATHEMATICA software, as $\lambda_1 = -0.853$, $\lambda_2 = -0.3691$, $\lambda_3 = -0.0579$, $\lambda_4 = 0$. Therefore, the fundamental matrix F is calculated as

$$F(t) = \begin{bmatrix} 0.305e^{\lambda_1 t} & 0.466e^{\lambda_2 t} & -0.061e^{\lambda_3 t} & -0.006 \\ -0.861e^{\lambda_1 t} & 0.488e^{\lambda_2 t} & -0.215e^{\lambda_3 t} & -0.025 \\ 0.203e^{\lambda_1 t} & -0.268e^{\lambda_2 t} & 0.813e^{\lambda_3 t} & -0.998 \\ 0.353e^{\lambda_1 t} & -0.686e^{\lambda_2 t} & -0.537e^{\lambda_3 t} & -0.041 \end{bmatrix}.$$

Since, F is invertible for every value of t (see Ross [12] and Hartman [13]), in particular it is invertible at $t = 0$. Thus,

$$F(0)^{-1} = \begin{bmatrix} 1.0251 & -0.723 & 0.0042 & 0.180 \\ 1.335 & 0.35 & -0.0047 & -0.298 \\ -0.962 & -0.85 & 0.08 & -1.290 \\ -0.933 & -0.933 & -0.933 & -0.933 \end{bmatrix}.$$

Using these values in Eqn. (7), it is obtained that

$$\begin{bmatrix} C_p(t) \\ C_f(t) \\ C_b(t) \\ C_n(t) \end{bmatrix} = \begin{bmatrix} 0.305e^{\lambda_1 t} & 0.466e^{\lambda_2 t} & -0.061e^{\lambda_3 t} & -0.006 \\ -0.861e^{\lambda_1 t} & 0.488e^{\lambda_2 t} & -0.215e^{\lambda_3 t} & -0.025 \\ 0.203e^{\lambda_1 t} & -0.268e^{\lambda_2 t} & 0.813e^{\lambda_3 t} & -0.998 \\ 0.353e^{\lambda_1 t} & -0.686e^{\lambda_2 t} & -0.537e^{\lambda_3 t} & -0.041 \end{bmatrix} \begin{bmatrix} 1.0251 \\ 1.335 \\ -0.962 \\ -0.933 \end{bmatrix},$$

which gives

$$\begin{bmatrix} C_p(t) \\ C_f(t) \\ C_b(t) \\ C_n(t) \end{bmatrix} = \begin{bmatrix} 0.312e^{\lambda_1 t} + 0.622e^{\lambda_2 t} + 0.068e^{\lambda_3 t} + 0.005 \\ -0.882e^{\lambda_1 t} + 0.651e^{\lambda_2 t} + 0.206e^{\lambda_3 t} + 0.023 \\ 0.208e^{\lambda_1 t} - 0.357e^{\lambda_2 t} - 0.782e^{\lambda_3 t} + 0.931 \\ 0.361e^{\lambda_1 t} - 0.915e^{\lambda_2 t} + 0.516e^{\lambda_3 t} + 0.038 \end{bmatrix}. \tag{8}$$

Therefore, Eqn. (8) determines explicitly the analytic profiles of the radiotracer concentrations in all the compartments, and also gives the mathematical structure of the input function, $C_p(t)$.

2.2   Solution with Known Input

In this case, the input is taken as previously published (see Lau et al. [2], Tantawy and Peterson [3])

$$C_p(t) = (A_1 t - A_2 - A_3)e^{\lambda_1' t} + A_2 e^{\lambda_2' t} + A_3 e^{\lambda_3' t} \tag{9}$$

with $A_1 = 851.1$, $A_2 = 21.88$, $A_3 = 20.81$ [μCi/ml]; $\lambda_1' = -4.134$, $\lambda_2' = -0.1191$, $\lambda_3' = -0.0104$ [min^{-1}]. Since, the input $C_p(t)$, being known explicitly in this case, application of law of conservation of mass and the first-order kinetics on the compartmental model shown in Figure 1, yield a non-homogeneous system of three linear differential equations

$$\frac{dC_f(t)}{dt} = -(k_2 + k_3 + k_5)C_f(t) + k_4 C_b(t) + k_6 C_n(t) + k_1 C_p(t); \ C_f(0) = 0, \tag{10}$$

$$\frac{dC_b(t)}{dt} = k_3 C_f(t) - k_4 C_b(t); \ C_b(0) = 0, \tag{11}$$

$$\frac{dC_n(t)}{dt} = k_5 C_f(t) - k_6 C_n(t); \ C_n(0) = 0, \tag{12}$$

where $C_p(t)$ is given in Eqn. (9). This system is put in the matrix form as

$$\frac{dC(t)}{dt} = M'C(t) + I(t); \ C(0) = O, \tag{13}$$

where

$$C(t) = \begin{bmatrix} C_f(t) \\ C_b(t) \\ C_n(t) \end{bmatrix}, \ M' = \begin{bmatrix} -(k_2 + k_3 + k_5) & k_4 & k_6 \\ k_3 & -k_4 & 0 \\ k_5 & 0 & -k_6 \end{bmatrix}, \ I(t) = \begin{bmatrix} C_p(t) \\ 0 \\ 0 \end{bmatrix}$$

and O is the zero column-vector. Again, as in previous case, if $G(t)$ is the fundamental matrix corresponding to the homogeneous part of Eqn. (13), the solution (see Ross [12] and Hartman [13]) to this initial value problem is

$$C(t) = G(t)G(0)^{-1}C(0) + \int_0^t G(t)G(s)^{-1}I(s)ds$$

which gives

$$C(t) = \int_0^t G(t)G(s)^{-1}I(s)ds. \tag{14}$$

Eqn. (14) gives the explicit values of all the tracer-concentrations in the corresponding compartments in this case, which in-turn are used to evaluate other essential parameters required while obtaining PET data, as elaborated in the following case-study.

Case-Study:

In this case, the same set of values of transfer coefficients, $k_1 - k_6$ is considered as in previous case-study and the known input is taken as given by Eqn. (9). Therefore,

$$M' = \begin{bmatrix} -0.605 & 0.005 & 0.17 \\ 0.2 & -0.005 & 0 \\ 0.28 & 0 & -0.17 \end{bmatrix}.$$

The eigenvalues of M' are calculated as $\beta_1 = -0.696$, $\beta_2 = -0.081$, $\beta_3 = -0.0018$, so that the fundamental matrix $G(t)$ corresponding to the homogeneous part of Eqn. (13) is

$$G(t) = \begin{bmatrix} -0.855e^{\beta_1 t} & 0.236e^{\beta_2 t} & -0.015e^{\beta_3 t} \\ 0.247e^{\beta_1 t} & -0.620e^{\beta_2 t} & -0.999e^{\beta_3 t} \\ 0.454e^{\beta_1 t} & 0.747e^{\beta_2 t} & -0.026e^{\beta_3 t} \end{bmatrix}.$$

Hence, from Eqn. (14), it is obtained that

$$
\begin{aligned}
C_f(t) &= e^{-5.042t}[-48.64e^{4.92t} + 44.44e^{5.03t} + e^{0.9t}(12.13 - 241.99t) + e^{5.04t}(23.73 + 1.88t) \\
&\quad + e^{4.96t}(37.13 + 28.99t) + e^{4.34t}(-68.81 + 211.11t)],
\end{aligned}
\tag{15}
$$

$$
\begin{aligned}
C_b(t) &= e^{-5.042t}[85.33e^{4.92t} - 1588.15e^{5.03t} + e^{4.96t}(-97.55 - 76.16t) + e^{4.34t}(19.88 - 60.98t) \\
&\quad + e^{0.9t}(-0.58 + 11.70t) + e^{5.04t}(1581.08 + 125.44t)],
\end{aligned}
\tag{16}
$$

$$
\begin{aligned}
C_n(t) &= e^{-5.04t}[-271.08e^{4.92t} + 76.7e^{5.03t} + e^{4.34t}(36.54 - 112.1t) + e^{5.04t}(41.14 + 3.26t) \\
&\quad + e^{0.9t}(-0.85 + 17.07t) + e^{4.96t}(117.54 + 91.76t)].
\end{aligned}
\tag{17}
$$

Thus, in this case, the radiotracer concentrations in each of the compartments are also determined explicitly.

3 Results

The solutions obtained in this model, depict explicitly and accurately the tracer concentrations in each of the compartments, while concerning with unknown as well as known inputs of the tracer material. The solutions are more general and authentic, and can be applied to any type of the injected radioactive tracer. Since, the parameters like the transfer coefficients, depend upon the type of the tracer, individual, *ROI* and many more factors. Thus, in each solution method, a particular case-study is considered.

Since, in each case-study, all the concentration-profiles, including the input function as well, are determined explicitly, these profiles are presented graphically in Figures 2–9. Figure 2 shows the variation of the input $C_p(t)$, determined in this work, with time as well as its comparison with the already published input. Clearly, the two inputs show a different behavior initially and then have the same structure and variation onwards, as their curves coincide thereafter.
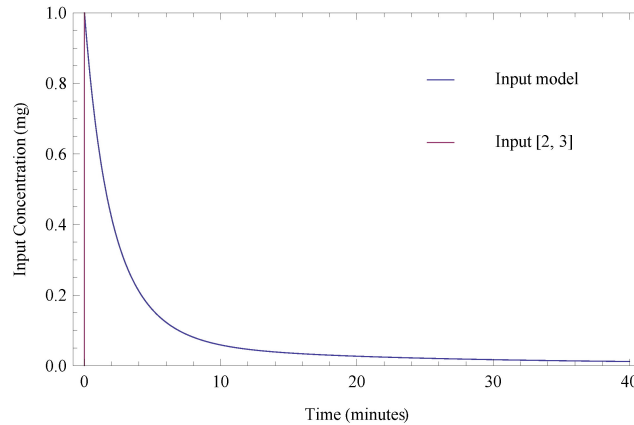

Figure 2: Comparison of the inputs $C_p(t)$ according to Eqn. (8) and $C_p(t)$ as per Eqn. (9) (see Lau et al. [2], Tantawy and Peterson [3]).

The other concentration profiles viz; $C_f(t)$, $C_b(t)$, and $C_n(t)$ are determined explicitly in both of the solutions used and are plotted in Figures 3 and 4, respectively. As shown, these concentrations, depicted using the solutions of this work, increase slightly up-to some peak and thereafter start decaying, which is also described in other works from the literature (see Lau et al. [2], Logan [4] and Phair [9]), which depict the accuracy of the solution presented in this work.
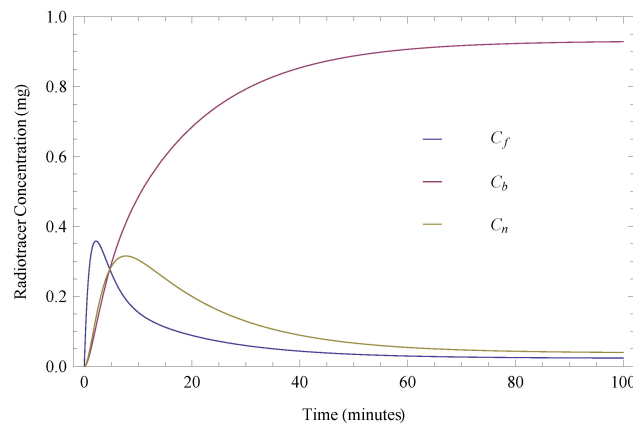

Figure 3: Time-activity profiles $C_f(t)$, $C_b(t)$, $C_n(t)$ of the radiotracer according to Eqn. (8).

The most important concentration-profile C_{PET} is also determined explicitly using both the solutions. The importance of this profile is that the data obtained by the PET camera during scanning is approximated to this profile as it is the summation of the other profiles (see Watabe et al. [5]), given as:
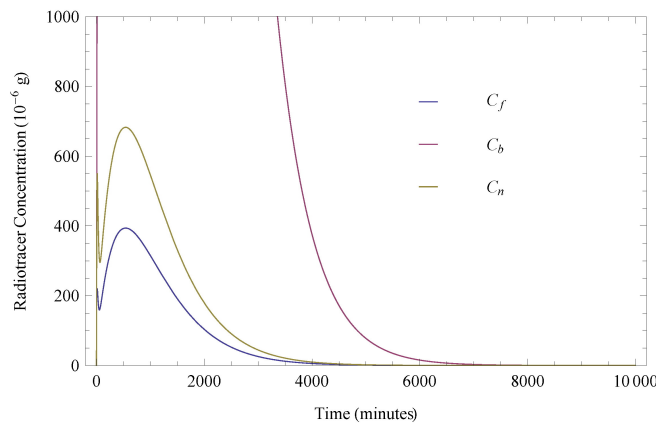
$$C_{PET}(t) = C_f(t) + C_b(t) + C_n(t).$$

Figure 4: Time-activity profiles $C_f(t)$, $C_b(t)$, $C_n(t)$ of the radiotracer according to second solution with known-input given by Eqns. (15)- (17)

Using this equation, the C_{PET}-profiles determined, using both the solutions, are presented graphically in Figures 5 and 7.
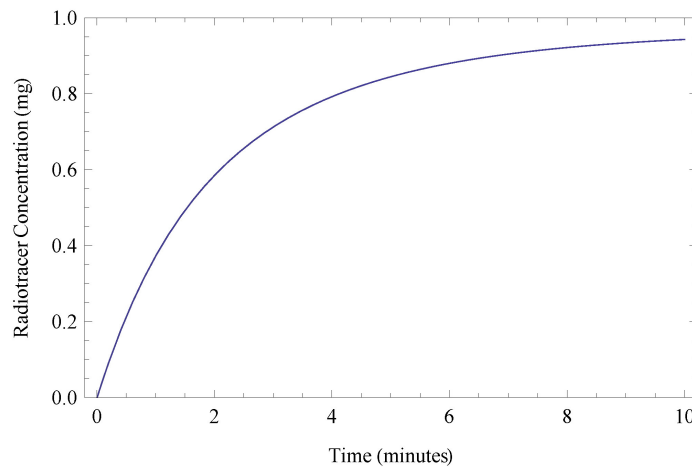

Figure 5: $C_{PET}(t)$ concentration-profile obtained as a summation of $C_f(t)$, $C_b(t)$, and $C_n(t)$ using Eqn. (8).

Finally, in order to check the accuracy of the obtained solutions, comparisons of the concentration-profiles are presented in Figures 8 and 9. The profile $C_b(t)$ is compared to the same profile mentioned in the work of Logan [4] as shown in Figure 8, where it is clearly visible that both the $C_b(t)$-profiles converge quite accurately. Moreover, the $C_{PET}(t)$-profile obtained using the solution with unknown input is compared to the work of Phair [9], by interpolating his data in our solution, showing initially the two profiles are different, and thereafter are quite much converging.

Using the explicit values of these concentration-profiles, one can easily determine the other essential parameters required in PET during scanning and diagnosis like the standardized uptake value (SUV), fractional uptake rate (FUR), and the distribution volume (DV). For the definitions of these terms see Logan [4], Bentourkia and Zaidi [6].
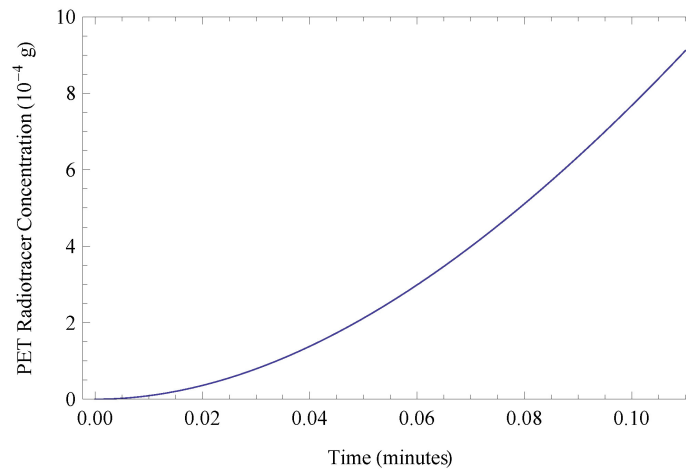
Figure 6: $C_{PET}(t)$ concentration-profile obtained as a summation of $C_f(t)$, $C_b(t)$, and $C_n(t)$ using Eqn. (8).
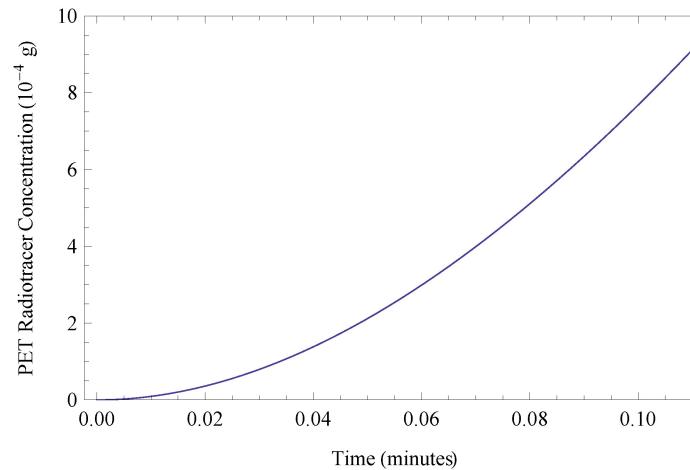

Figure 7: $C_{PET}(t)$ concentration-profile obtained as a summation of $C_f(t)$, $C_b(t)$, and $C_n(t)$ using Eqns. (15)–(17).

4   Discussion and Conclusion

This work presents two new solutions of a frequently used compartmental model in tracer kinetic modeling of PET. The model solutions are obtained for two cases; one with an unknown input and the other with a known input, which can be applied to various PET data. The solutions are obtained using the fundamental matrix method for homogeneous and non-homogeneous system of linear ordinary differential equations, respectively. The first solution, where the input is not known, depicts the radiotracer-concentrations explicitly, as well as determines the input function. Thus, this solution has the benefit in itself for constructing the input function. In the second case, the concentrations are also determined explicitly using a known-input function.

The solutions can be used to any type of tracer or individual under diagnosis in PET. The only thing that has to be changed, in these solutions, is the numerical values of the transfer coefficients occurring in the model as their values depend upon the tracer type, and individual's *ROI* under diagnosis. Furthermore, the solution-methods presented in this work can be used to any type of linear compartmental model used in kinetic modeling of PET.

The solutions are easy to evaluate and more accurate than previously determined solutions. Therefore,
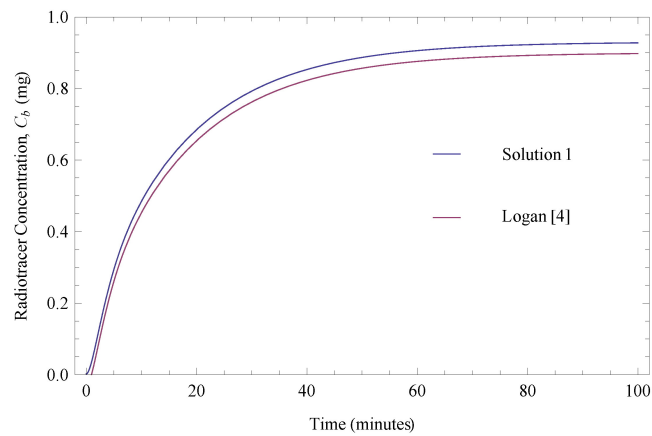
Figure 8: Comparison of the concentration-profile $C_b(t)$, given in Eqn. (8) with that of the mentioned in the work of Logan [4].
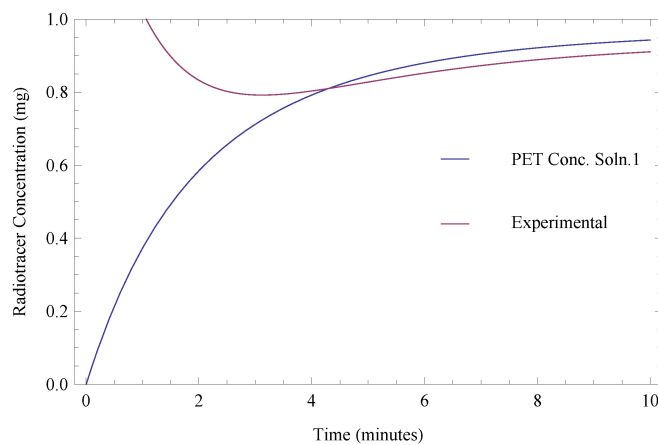

Figure 9: Comparison of the concentration-profile $C_{PET}(t)$, obtained using Eqn. (8) with that of the mentioned in the work of Phair [9].

in terms of the accuracy, the explicit derivations of all the tracer-concentration-profiles are accurate. From these profiles, all the other essential parameters required, while obtaining and studying PET data, are also evaluated easily with more accuracy and precision. Since, the information regarding the input function, is crucial and vital in PET kinetic modeling, the main achievement in this work is the determination of the input function, which represents the delivery of the radiotracer to a site of interest. In this way, the work is applicable in nuclear medicine and other imaging studies used for diagnosis of various diseases, and tracking the progress of other physiological processes of human body, scanned through PET.

This work can further be extended in several ways viz; by considering some other compartmental models having more than four compartments, by considering the transfer-coefficients as variables, by using the second and higher order kinetic-principles.

References

[1] N. A. Peppas and B. Narasimhan, Mathematical models in drug delivery: How modeling has shaped the way we design new drug delivery systems, Journal of Controlled Release, 190 (2014), 75–81.

[2] C. H. Lau, D. Feng, B. F. Hutton, D. Pak-Kong Lun and W. C. Siu, Dynamic imaging and tracer kinetic modeling for emission tomography using rotating detectors, IEEE Transactions on Medical Imaging, 17(1998), 986–994.

[3] M. N. Tantawy and T. E. Peterson, Simplified [^{18}F]FDG image-derived input function using the left ventricle, liver and one venous blood sample, Mol. Imaging, 9(2010), 76–86.

[4] J. Logan, Graphical analysis of PET data applied to reversible and irreversible tracers, Nuclear Medicine and Biology, 27(2000), 661–670.

[5] H. Watabe, Y. Ikomo, M. Naganawa and M. Shidahara, PET kinetic analysis-compartmental model, Annals of Nuclear Medicine, 20(2006), 583–588.

[6] M. Bentourkia and H. Zaidi, Tracer kinetic modeling in PET, PET Clinics, 2(2007), 267–277.

[7] K. T. Nguyen, A. Bock, A. Ynnerman and T. Ropinski, Deriving and visualizing uncertainty in kinetic PET modeling, Eurographics Workshop on Visual Computing for Biology and Medicine, (2012).

[8] O. N. Shevtsova and V. K. Shevtsova, Mathematical simulation of transport kinetics of tumor-imaging radiopharmaceutical ^{99m}Tc-MIBI, Comput. Math. Methods Med., (2017), 1–12.

[9] R. D. Phair, Differential equation methods for simulation of GFP kinetics in non-steady state experiments, Molecular Biology of the Cell, 29(2018), 763–771.

[10] https://en.wikipedia.org/wiki/Radioactive_tracer

[11] https://www.radiologyinfo.org/en/info.cfm?pg=gennuuclear

[12] S. L. Ross, Differential Equations, WILEY, 3, 2007.

[13] P. Hartman, Ordinary Differential Equations, Classics in Applied Mathematics, 2002.